Contributions to Cable Constants Programs for Accurate and Efficient Electromagnetic Transient Modeling in Submarine Cables

D. L. Pires, F. A. Moreira, M. G. Soares, F. M. Vasconcellos

***Abstract*—This paper presents the implementation of two proposals designed to enhance computational accuracy and efficiency in the simulation and modeling of cables within Cable Constants Programs. The first proposal involves the optimized application of the numerical method known as the Double Exponential formula for solving improper integrals related to ground-return parameters, which are essential for determining the per-unit-length impedance and admittance. These parameters are particularly significant when dealing with specific soil characteristics, such as those found in marine environments. The second proposal is the use of the Singular Value Decomposition method for computing eigenvector matrices required for determining the propagation function and characteristic admittance, both crucial for transient analysis. Two case studies, involving Single-Core HVDC Cables and Pipe-Type Cables, demonstrated promising results. For both cases, the behavior of the analyzed parameters was compared with conventional methodologies over a wide frequency spectrum. The results were presented in graphs and evaluated using quantitative metrics such as Mean Squared Error and Mean Relative Error. Findings indicate that both proposals are less sensitive to irregularities in functions and ill-conditioned matrices, exhibiting good performance and demonstrating their potential as robust techniques to be utilized and explored for such applications.**

***Keywords*—Cable Constants Program, Ground-Return Parameters, Numerical Integration, Per-unit-length Parameters, Singular Value Decomposition, Submarine Cable Modeling.**

I. Introduction

THE growing demand for energy transmission has driven significant advancements in the use of submarine cable systems beneath the ocean floor. These systems are essential for applications such as connecting offshore wind farms to continental grids, supporting offshore petrochemical facilities, and linking power networks between islands and countries [1], [2], [3].

Consequently, the accurate determination of the distributed parameters that model these cables is of paramount technical importance [4], [5]. These parameters refer to the per-unit-length impedance $\mathbf{Z}$ and admittance $\boldsymbol{Y}$ matrices, which are fundamental for obtaining the characteristic admittance $\boldsymbol{Y_c}$ and the propagation $\mathbf{H}$ matrices, key elements in the simulation of electromagnetic transients.

These parameters are obtained through computational routines implemented in simulation software, commonly referred to as Line/Cable Data (LCD), Line Constants Program (LCP), or Cable Constants Program (CCP). The primary goal of such programs is to compute the impedance and admittance matrices based on the cable's characteristics and the surrounding medium, accounting for effects such as skin, proximity, and ground return.

The classical method involves constructing these matrices by summing the individual contributions of these effects, while considering the structural aspects of the cable (or multiple cables) and the electrical and magnetic properties of the propagation medium [6].

In recent years, important advancements have emerged in this field, introducing more detailed formulations. These include the consideration of non-homogeneous soils, multiple propagation media, proximity effects, and ground return admittance effects [7], [8], [9], [10], [11]. Alternative methods for calculating these matrices include the finite element method (FEM) and the method of moments with surface admittance operator (MoM-So) [12], [13], [14], both based on a more complete electromagnetic theory. Although highly accurate, these methodologies involve greater mathematical complexity and demand careful numerical treatment of the external medium representation [11].

In this context, the construction of per-unit-length parameter matrices is highly sensitive and influenced by several factors, such as the need for inverting large matrices, solving improper integrals, and handling Bessel functions that can become unstable at high frequencies [6], [10]. These procedures must be carefully executed, especially when the goal is to ensure the accuracy of electromagnetic transient simulations and enhance the reliability of analyses.

This demands a careful analysis of each situation, avoiding analytical approximations, firstly, in determining ground-return parameters in cases where their applicability limits are exceeded [15]. Such cases often involve cables buried at significant depths and/or separated by large distances, as in offshore oil and gas production systems, specific HVDC transmission scenarios, or high-resistivity environments where seabed conditions can vary due to uncommon soil types [16].

This work was supported by Coordenação de Aperfeiçoamento de Pessoal de Nível Superior - Brasil (CAPES) - Código 001.

D. L. Pires is with the Federal University of Bahia (UFBA) and the Federal Institute of Bahia (IFBA), Salvador, BA, Brazil (e-mail: davidpires@ufba.br). F. A. Moreira is with the Department of Electrical and Computer Engineering of the Federal University of Bahia (UFBA), Salvador, BA, Brazil (e-mail: moreiraf@ufba.br). M. G. Soares is with the Department of Engineering and Computing of the State University of Santa Cruz (UESC), Ilhéus, BA, Brazil (e-mail: mgsoares@uesc.br). F. M. Vasconcellos is with the Department of Electrical Engineering of the Federal University of Bahia (UFBA), Salvador, BA, Brazil (e-mail: felipe.vasconcellos@ufba.br).

Paper submitted to the International Conference on Power Systems Transients (IPST2025) in Guadalajara, Mexico, June 8-12, 2025.

Moreover, when the calculation of the characteristic admittance and propagation matrices is required, it becomes necessary to compute matrices composed of eigenvectors (transformation matrices) and their associated eigenvalues.

This second process is non-trivial, particularly in systems that may produce ill-conditioned matrices. In certain cases, artificial oscillations or coalescence of eigenvalues can occur, leading to significant inaccuracies in transient simulations [11]. This study proposes procedures to address these two critical challenges in Cable Constants Programs. Both approaches primarily aim to enhance simulation accuracy, with improved system reliability, reduced costs in project design and maintenance, and other substantial benefits to the industry as secondary outcomes.

The first proposal concerns the accurate calculation of ground-return parameters without compromising computational efficiency. The proposal involves the development of an algorithm based on the numerical integration method known as the Double Exponential (DE) formula to compute the improper integrals related to these parameters, avoiding the use of analytical approximations. This procedure is related to the calculation of $\mathbf{Z}$ and $\mathbf{Y}$.

The second proposal refers to the accurate calculation of transformation matrices, eliminating instabilities and unwanted oscillations. An algorithm is suggested for the explicit calculation of eigenvalues, along with the use of the Singular Value Decomposition (SVD) method to identify these matrices. This procedure is related to the determination of $\boldsymbol{Y_c}$ and $\mathbf{H}$, assuming that the per-unit-length impedance and admittance have been properly obtained.

The paper is organized as follows: Section II details the structure of the Cable Constant Program, addressing the theoretical considerations adopted for calculating the per-unit-length parameter matrices, as well as the post-processing required to determine the characteristic admittance and propagation matrices. Section III presents the methodology used for the application of the Double Exponential formula, proposed to compute the integrals related to the return parameters, with test cases demonstrating the validity of the formulation. Section IV suggests an optimized use of the SVD method for calculating transformation matrices, also validated through comparative test cases. Finally, Section V presents the conclusions of this work.

II. Cable Constants Program

A. Per-Unit-Length Impedance and Admittance

This study takes into account the skin and the ground-return effects in the cable modeling, as well as a propagation model with a non-homogeneous soil consisting of two layers, with the cable placed in the second layer. Additionally, the Single-Core Coaxial Cable (SC) and Pipe-Type Cable (PT) are analyzed, as they are commonly used in power line applications [17].

For the determination of impedance and admittance in SC cables, the following formulations are considered. In these equations, the indices i and o refer to the internal and external media impedance/admittance, respectively. Specifically, **Pi** and **Po**, the potential coefficient matrices, are related to the insulation layers and the representation of the external media shunt admittance, respectively.

$$\mathbf{Z} = \mathbf{Z_i} + \mathbf{Z_o} \tag{1}$$

$$\mathbf{Y} = j\omega(\mathbf{P_i} + \mathbf{P_o})^{-1} \tag{2}$$

For PT cables, the following formulations are considered. In this case, the indices "p" and "c" represent the pipe internal impedance/admittance and the connection impedance/admittance between the inner and outer surfaces, respectively.

$$\mathbf{Z} = \mathbf{Z_i} + \mathbf{Z_p} + \mathbf{Z_c} + \mathbf{Z_o} \tag{3}$$

$$\mathbf{Y} = j\omega(\mathbf{P_i} + \mathbf{P_p} + \mathbf{P_c} + \mathbf{P_o})^{-1} \tag{4}$$

Part of this formulation is based on a classical reference still used nowadays [6]. This part includes the representation of the internal impedance and admittance for both types of cables, accounting for the skin effect and considering multiple conductive and insulating layers, each with specific electrical and magnetic characteristics and described geometrically. Additionally, for PT cables, the influence of the pipe is included in the calculation of the total impedance and admittance. The equations for calculating all these parameters are well known and therefore have been omitted.

The equations adopted in this work differ from those presented in [6] due to the inclusion of updated considerations in the representation of the external medium. Generally, the equation proposed by Pollaczek [18] or its generalizations are used. Another option is the use of approximate analytical equations, such as those proposed in [19].

In this work, the formulation based on [10] was adopted. According to the equations below, for the calculation of **Zo** and **Po**, a double-layer earth is considered, with the cable placed in the second medium, making the formulation more accurate by not neglecting the propagation effect due to the influence of medium 1 along the cable axis and avoiding the use of analytical approximations. Specifically, for the calculation of **Po**, it is considered that displacement currents should not be neglected.

$$\mathbf{Z_{o(m,n)}} = \frac{j\omega\mu_0}{2\pi}[K_0(\gamma_1 d) - K_0(\gamma_1 D) + 2\int_0^\infty \frac{e^{-(h_m+h_n)u_1}}{u_1+u_0} cos(r\lambda)d\lambda] \tag{5}$$

$$\mathbf{P_{o(m,n)}} = \frac{j\omega}{2\pi(\sigma_1+j\omega\epsilon_1)}[K_0(\gamma_1 d) - K_0(\gamma_1 D) + 2\int_0^\infty \frac{u_0}{u_1}\left[\frac{e^{-(h_m+h_n)u_1}}{u_0+\gamma_0^2\gamma_1^{-2}u_1}\right] cos(r\lambda)d\lambda] \tag{6}$$

$$\mathbf{Y_o} = j\omega\mathbf{P_o^{-1}} \tag{7}$$

In these equations, **Zo** refers to the ground-return impedance, while **Po** represents the ground-return potential coefficient, necessary for calculating the ground return admittance **Yo**. Equations (5) and (6) refer to the mutual parameters. For the calculation of the self-parameters, simply set $h_m = h_n$ and $r = r_{ext}$, where r_{ext} is the radius of the outermost layer of the cable. Additionally, the indices m and n refer to the generic set of two cables, with h_m and h_n representing the depth of each cable measured from their respective centers. The r represents the horizontal distance separating the cable centers, and the distance-related auxiliary parameters d and D are given by: $d = \sqrt{(h_m - h_n)^2 + r^2}$ and $D = \sqrt{(h_m + h_n)^2 + r^2}$.

Additionally, the indices 0 and 1 refer to the propagation media present in the model. In the case studied, "0" refers to the sea and "1" refers to the seabed. Complementarily, ω is the angular frequency of the system, and σ and ϵ represent, respectively, the electrical conductivity and permittivity of the medium, and μ represents the magnetic permeability of the medium. The propagation constant of the medium is given by $\gamma = \sqrt{j\omega\mu(\sigma + j\omega\epsilon)}$. Finally, K_0 refers to the modified Bessel function of the second kind with zero order and the auxiliary parameter u is given by $u = \sqrt{\lambda^2 + \gamma^2}$.

B. Characteristic Admittance and Propagation Function

After calculating the **Z** and **Y** matrices, the procedure for identifying $\boldsymbol{Y_c}$ and **H** involves solving the equations below, such that **Tv** and **Ti** are the eigenvector matrices of the products $\mathbf{Z} \cdot \mathbf{Y}$ and $\mathbf{Y} \cdot \mathbf{Z}$, respectively, and l is the cable length [11]. The square root of these products may yield multiple solutions. Therefore, a modal transformation is applied in order to find a coordinate system where $\mathbf{Z} \cdot \mathbf{Y}$ and $\mathbf{Y} \cdot \mathbf{Z}$ are diagonal.

$$\mathbf{Y_c} = \mathbf{T_v} \cdot \left(\mathbf{Z_{mode}^{-1}} \sqrt{\mathbf{Z_{mode}} \cdot \mathbf{Y_{mode}}} \right) \cdot \mathbf{T_v^T} \tag{8}$$

$$\mathbf{H} = \mathbf{T_v} \cdot \exp\left(-\mathrm{l} \sqrt{\mathbf{Z_{mode}} \cdot \mathbf{Y_{mode}}} \right) \cdot \mathbf{T_v^{-1}} \tag{9}$$

$$\mathbf{Z_{mode}} = \mathbf{T_v^{-1}} \cdot \mathbf{Z} \cdot \mathbf{T_i} \tag{10}$$

$$\mathbf{Y_{mode}} = \mathbf{T_i^{-1}} \cdot \mathbf{Y} \cdot \mathbf{T_v} \tag{11}$$

III. Optimized Double Exponential formula for calculating ground-return parameters

The Double Exponential formula is a numerical method originally proposed in [20], designed to find an approximate solution to an integral, making it a suitable option for calculating the integrals involved in the return parameters. In the following equation, x_k represents the abscissas, w_k the weights and k defines both the summation limits and each individual term of the summation.

$$\int_{-1}^{1} f(x)dx \approx \sum_{k=-\infty}^{\infty} w_k f(x_k) \tag{12}$$

Additionally, the method employs hyperbolic functions to determine the abscissas and weights, while also suggesting a change in the integration interval [21]. Specifically, this work adopts the Tanh-Sinh quadrature due to its robustness and efficiency, as one of the method's key features is its rapid convergence. After applying the integral transformation, the transformed function exhibits a double-exponential decay [22]. The Tanh-Sinh quadrature, originally introduced in [20], is implemented in this study as outlined in the following equations. The procedure for applying the method to equations (5) and (6) is described in the Appendix.

$$x_k = tanh\left[\frac{1}{2}\pi sinh(kh)\right] \tag{13}$$

$$w_k = \frac{\frac{1}{2}h\pi cosh(kh)}{cosh^2\left[\frac{1}{2}\pi sinh(kh)\right]} \tag{14}$$

The interval k must be chosen to ensure that no relevant terms are omitted in the integral calculation. The step size h is associated with the number of subdivisions of the integration interval and, consequently, with the accuracy of the calculation. An efficient approach would be to determine an optimal relationship between these parameters to avoid unnecessary computational effort.

A. Proposed Methodology

The definition of the parameters k and h is the key to achieving both accuracy and efficiency in the solution. In [22], it is suggested to use the concept of levels to determine the step size, with $h = 2^{-m}$, where $m = [1, 2, 3, 4, \dots]$. Next, an initial guess for the range of k is defined, and the problem is solved. In [21], it is stated that there are two sources of error in the approximation: error from truncation and error from discretization. These errors become larger if the integrand decay is too fast or too slow, respectively.

To minimize these errors, it is suggested to find an expression that relates k and h, starting from the formulation that both errors must be equal. The goal is to achieve a balanced solution in terms of the impacts caused by these errors. In [21], the author proposes $k = \left(\frac{1}{2h}\right) \log\left(\frac{2\pi}{h}\right)$.

Fig. 1 shows a flowchart illustrating the methodology proposed in this work to apply the method while avoiding unnecessary computational effort. The approach starts with the initial concept of levels, prioritizing the increase of the range k over the increase in levels, as the latter significantly raises computational cost. By increasing k, the idea is to converge to the desired solution, advancing the level only if the problem's solution does not satisfy the predefined tolerance 10^{-p}, where p represents the desired number of precision digits. If p increases to exceed an established limit, increasing the level becomes a better option. In this work, the adopted limit was $lim = 50$.

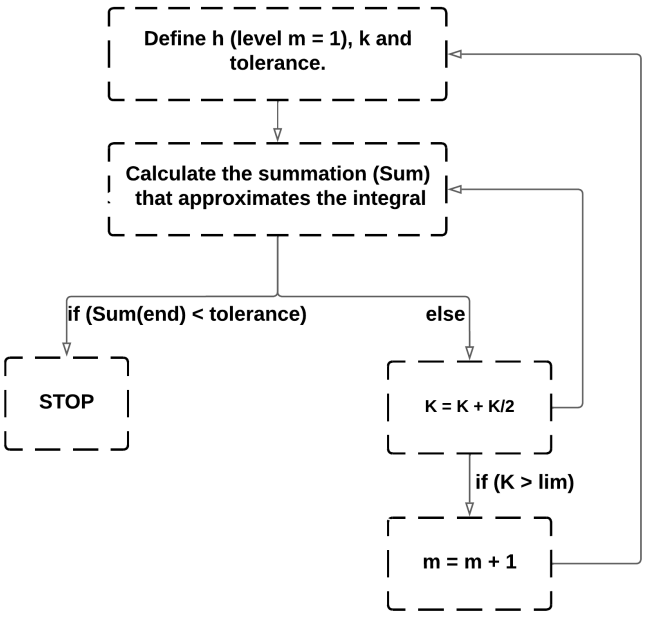

Fig. 1. Flowchart for Implementing the DE Method.

B. Test Case

To validate the results obtained from applying the proposed methodology, a program was developed using MATLAB (Matrix Laboratory). The goal is to analyze the behavior of the ground-return parameters over a wide frequency range, representing the main electromagnetic transient phenomena (10 - 10^7) Hz. Fig. 2 shows the simulated system, which consists of two SC HVDC cables buried in the seabed. Each cable includes a core, inner insulation, lead sheath, and outer insulation. In this case, the adopted parameters were $h_m = h_n = 1$m and $r = 1$m.

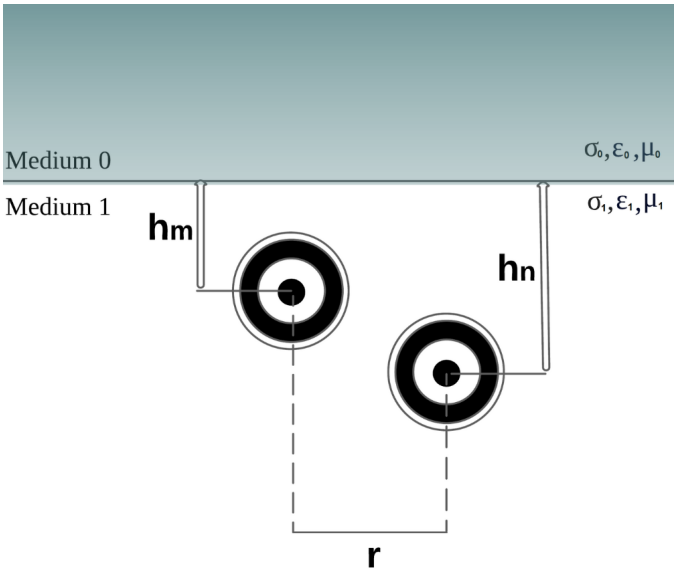

Fig. 2. Test Case: Two SC HVDC Cables.

Data regarding the characteristics of each medium is presented in Table I, along with the geometric, electrical, and magnetic parameters of each cable layer [9]. The symbols $r_1 - r_4$ represent the radius of each layer related to the cable's center, while ρ, ϵ, and μ denotes the resistivity, electrical permittivity, and magnetic permeability of each layer, respectively.

TABLE I
SEA/SEABED AND SC CABLE PARAMETERS

Medium	σ (S/m)	ϵ (F/m)	μ (H/m)
Sea (0)	5	$81\epsilon_0$	μ_0
Seabed (1)	1.5	$40\epsilon_0$	μ_0
Outer Radius (mm)	ρ (Ωm)	ϵ (F/m)	μ (H/m)
$r_1 = 33.95$	$1.7e-8$	-	μ_0
$r_2 = 60.65$	-	$3.5\epsilon_0$	μ_0
$r_3 = 64.65$	$21e-8$	-	μ_0
$r_4 = 71.05$	-	$8\epsilon_0$	μ_0

As a benchmark for comparison, the closed-form equations (CF) proposed in [15], derived from [10], were employed. Although there are applicability limits concerning vertical distances ($h_m, h_n \leq 1$m) and horizontal distances ($r \leq 2$m), these limits are not violated in the tested case [15]. Additionally, the Gauss-Laguerre (GL) numerical integration method was used for comparison purposes to highlight the advantages of the Double Exponential (DE) method.

Finally, the global adaptive quadrature method available in the MATLAB function *integral* (INT) was also employed. The purpose of this approach is to assess the performance of the other methods using an external reference, given that they were obtained through distinct formulations, whereas INT is a built-in MATLAB function.

Fig. 3 and Fig. 4 illustrate the real and imaginary parts of the self ground-return parameters for both impedance and admittance. Similarly, Fig. 5 and Fig. 6 present the real and imaginary parts of the mutual ground-return parameters. It can be observed that across the frequency range, the DE method aligns closely with the CF and INT method. This occurs because the DE method demonstrates strong convergence when handling integrands that cannot be expressed as finite combinations of algebraic functions like polynomials and exponentials.

Certain functions may exhibit restrictions in their smoothness, such as irregularities or abrupt changes. The DE method performs well in handling such functions because it maps the integration interval into a finite range where the integrand exhibits a simpler behavior [22]. Moreover, a similar result between DE and CF is expected since the closed-form equations were developed considering the asymptotic approximation of the equations proposed in [10], which are the same ones adopted in this work.

On the other hand, the GL method converges only when the function forming the integrand is sufficiently smooth. It can be stated that the degree of smoothness allows the function to be approximated by a polynomial. In cases where this is not possible, the GL method may diverge even when its input parameters (such as quadrature points, polynomial degree, etc.) are adjusted [23]. Such cases can arise due to a combination of factors, including the characteristics of the medium where the

cable is located, the burial depth of the cable, and the distance between cables. This highlights the importance of selecting the appropriate numerical integration method depending on the system being analyzed.

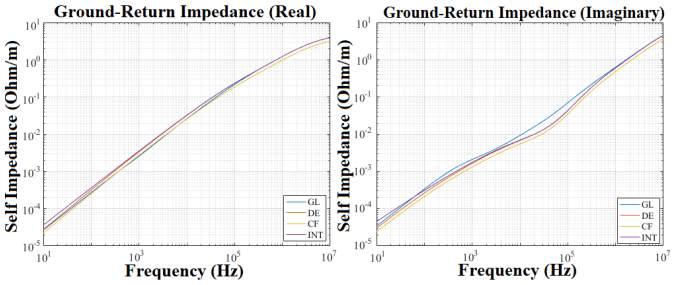

Fig. 3. Ground-Return Self Impedance for DE, GL, INT and CF methods.

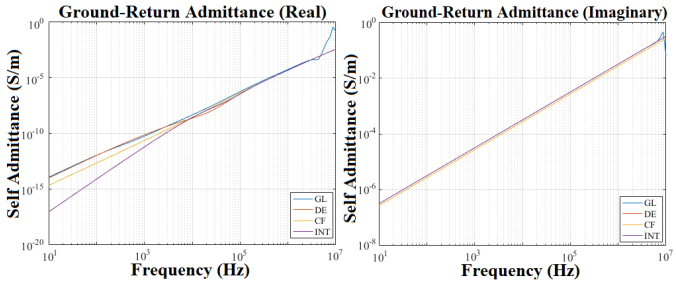

Fig. 4. Ground-Return Self Admittance for DE, GL, INT and CF methods.

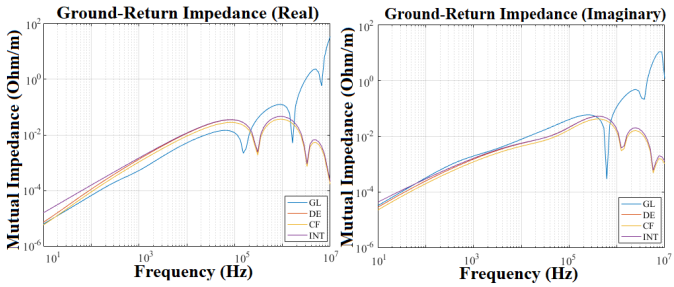

Fig. 5. Ground-Return Mutual Impedance for DE, GL, INT and CF methods.

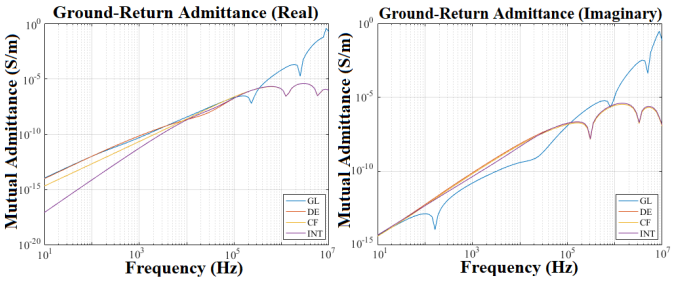

Fig. 6. Ground-Return Mutual Admittance for DE, GL, INT and CF methods.

Table II presents the elapsed time for simulating the self and mutual components of impedance and admittance using each method, as well as the mean squared error (MSE) of the results obtained from the DE, GL and INT methods when compared to the CF method. The elapsed time was computed using the *tic* and *toc* functions in MATLAB. In terms of accuracy, the performance of the DE, INT and CF methods is similar. Regarding efficiency, the CF method performs better, although the DE and INT methods also deliver results within a few seconds.

TABLE II
SIMULATION TIME AND MEAN SQUARED ERROR (MSE)

-	DE	GL	INT	CF
Simulation Time (Z)	5.03s	43.81s	0.44s	0.02s
Simulation Time (Y)	7.12s	45.64s	0.53s	0.02s
MSE (Z_{self})	0.000027	0.000067	0.000029	-
MSE (Z_{mutual})	0.000007	83.389455	0.000008	-
MSE (Y_{self})	4.3e-11	0.001191	4.3e-11	-
MSE (Y_{mutual})	0.35e-16	0.002657	0.32e-16	-

Two interesting cases can be observed in Fig. 7 and Fig. 8. For the first case, $h_m = h_n = 1.2m$ and $r = 3m$, representing parameters that exceed the applicability limits of the CF method, as suggested in [15]. Specifically, when calculating the mutual parameters, discrepancies between the results from the DE/INT and CF methods were observed along the frequency range.

This also occurs in case 2, where a soil resistivity of $500\Omega m$ was adopted to analyze less conductive media. In this case, the results obtained from DE/INT also slightly differ from those of the CF method, particularly for impedance. This was expected since there is a relationship between increasing soil resistivity and the accuracy of the impedance closed-form equations, including the observation that no clear correlation was identified between ground-return admittance accuracy and ground resistivity, as highlighted in [15], except at very high frequencies.

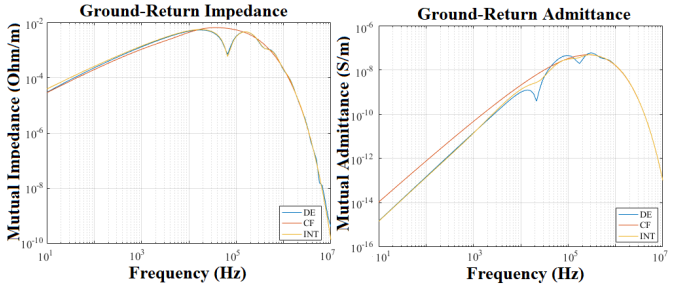

Fig. 7. Mutual Ground-Return Parameters (Case 1).

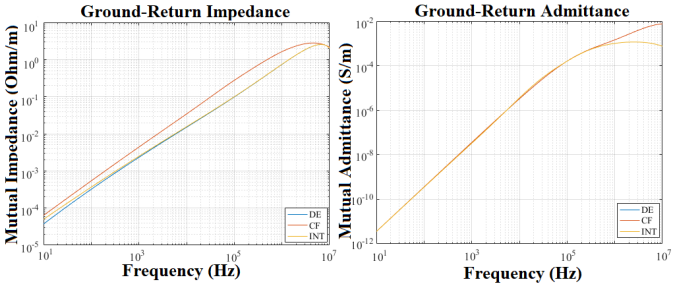

Fig. 8. Mutual Ground-Return Parameters (Case 2).

Tables III and IV detail the simulation elapsed time for each method and the Mean Relative Error (MRE) of the CF and INT methods compared to DE, for both particular cases. All results presented in the tables of this section consider the absolute values of the quantities when calculating the error.

TABLE III
SIMULATION TIME AND MEAN RELATIVE ERROR (MRE) - CASE 1.

-	DE	INT	CF
Simulation Time (Z_{mutual})	11.27s	0.44s	0.02s
Simulation Time (Y_{mutual})	19.01s	0.53s	0.02s
MRE (Z_{mutual})	-	0.153125	0.999214
MRE (Y_{mutual})	-	0.308870	2.255165

TABLE IV
SIMULATION TIME AND MEAN RELATIVE ERROR (MRE) - CASE 2.

-	DE	INT	CF
Simulation Time (Z_{mutual})	15.93s	0.58s	0.02s
Simulation Time (Y_{mutual})	17.09s	0.66s	0.02s
MRE (Z_{mutual})	-	0.063300	0.998427
MRE (Y_{mutual})	-	0.065215	0.680432

IV. OPTIMIZED SVD FOR CALCULATING TRANSFORMATION MATRICES

For calculating the parameters previously shown in (8) and (9), it is essential to obtain the transformation matrix **Tv** with high accuracy. This process directly depends on the accurate computation of the **Z** and **Y** matrices but extends beyond that. Calculating eigenvector matrices can be non-trivial in certain scenarios, such as when the matrix elements depend on frequency or in the presence of coalescing eigenvalues [11]. In such cases, inaccuracies arise, leading to **H** and $\boldsymbol{Y_c}$ matrices with oscillating elements. The ultimate consequence is inaccurate simulation of transient phenomena.

In this context, implicit calculations that rely on pre-defined functions may be prone to errors in specific situations like these. An open solution is proposed, involving the explicit computation of eigenvalues followed by the determination of the eigenvector matrix using the Singular Value Decomposition (SVD) technique.

A. Proposed Methodology

The proposed methodology consists of explicitly calculating the eigenvalues and eigenvectors to control numerical approximations and instabilities. First, the general equation $(\mathbf{A}-\lambda\mathbf{I})\mathbf{v}=0$ is solved, where $\mathbf{A}=\mathbf{Z}\cdot\mathbf{Y}$, λ is the eigenvalue vector, **I** is the identity matrix of the same dimension as **Z** and **Y**, and **v** is the eigenvector matrix that satisfies the general equation.

Fig. 9 shows a summary of the proposed methodology. Following the flowchart, for the calculation of λ it is suggested to first generate the coefficients of the characteristic polynomial and then calculate its roots. Once this is done, assuming $\mathbf{B}=\mathbf{A}-\lambda\mathbf{I}$, the SVD function is used to find the solution $\mathbf{B}\cdot\mathbf{v}=0$. The first column of the eigenvector matrix, **Tv**, is given by the last column of the matrix **v**. Finally, this process is repeated for each of the previously calculated eigenvalues, constructing the complete matrix **Tv**.

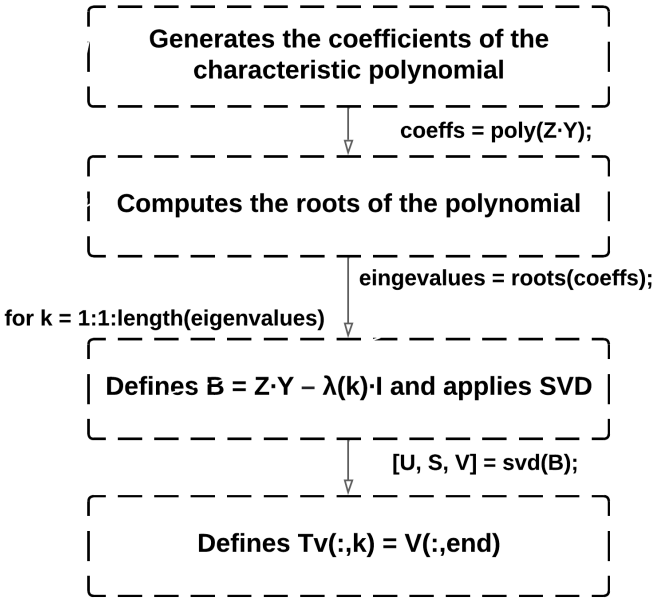

Fig. 9. Flowchart for Implementing SVD.

This can be understood by recognizing that the SVD decomposes the matrix **B** into the form given by the following equation, where **U** and **V** are orthogonal matrices, and $\boldsymbol{\Sigma}$ is a diagonal matrix whose diagonal values are the singular values of **B**, arranged in descending order [24].

$$\mathbf{B}=\mathbf{U}\boldsymbol{\Sigma}\mathbf{V}^{\mathbf{T}} \tag{15}$$

In summary, the smallest singular value of **B** indicates a direction where $\mathbf{B}\cdot\mathbf{v}$ is minimal. This direction is given by the last column of **V** in the SVD, making it the most likely solution to $\mathbf{B}\cdot\mathbf{v}=0$. This is particularly useful for ill-conditioned or approximate systems [25].

B. Test Case

The purpose of this section is to validate the feasibility and reliability of the proposed methodology. Fig. 10 shows the system to be simulated. In this case, it is a PT cable, selected for being more sensitive to the ill-conditioning problem of the matrices involved [11]. Here, the optimized DE method was also used to compute the ground-return parameters, but the focus is on the post-processing step, specifically the computation of matrices $\boldsymbol{Y_c}$ and **H**. Regarding the sea and seabed parameters, the same data from Table I were used, with $h=1m$. Table V presents the parameters adopted for the PT cable. Each internal cable has four layers: core, insulation, sheath, and second insulation $(r1-r4)$. Additionally, $(r5-r7)$ represent the armour's inner and outer radius, as well as the armour insulation.

Figs. 11 and 12 show the behavior of elements in the seventh column of matrices **H** and $\boldsymbol{Y_c}$, comparing the eigenvectors computed using the SVD with those obtained via a conventional technique based on the QR algorithm, as implemented in the MATLAB function *eig*.

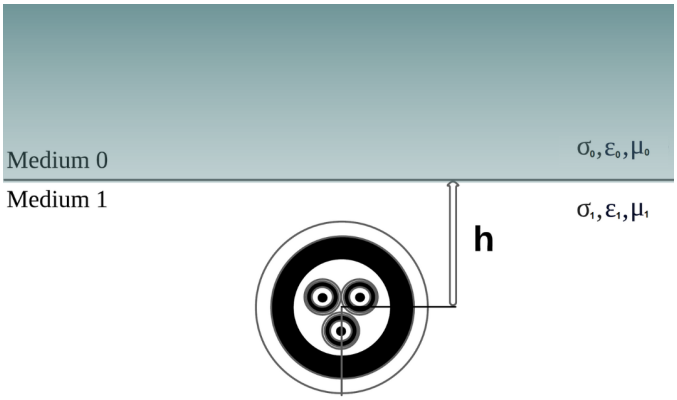

Fig. 10. Test Case: A Pipe-Type Cable.

TABLE V
PT CABLES PARAMETERS

Outer Radius (mm)	ρ (Ωm)	ϵ (F/m)	μ (H/m)
$r_1 = 9.6$	$1.7e-8$	-	μ_0
$r_2 = 17.054$	-	$3.31\epsilon_0$	μ_0
$r_3 = 18.054$	$22e-8$	-	μ_0
$r_4 = 19.50$	-	$2.3\epsilon_0$	μ_0
$r_5 = 48.00$	$2.86e-8$	$5\epsilon_0$	μ_0
$r_6 = 59.00$	-	-	$90\mu_0$
$r_7 = 65.00$	-	$10\epsilon_0$	μ_0

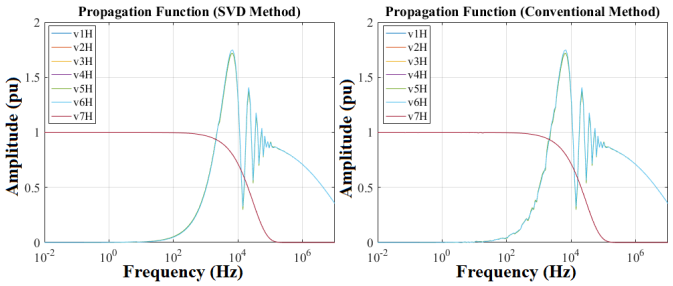

Fig. 11. Propagation Function for SVD and Conventional methods.

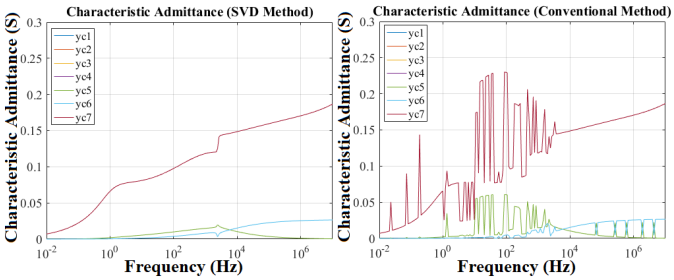

Fig. 12. Characteristic Admittance for SVD and Conventional methods.

It is noticeable that the conventional method exhibits a more oscillatory behavior, as it does not aim to provide greater control over numerical approximations. On the other hand, the SVD method smooths out these oscillations because, in constructing the eigenvector matrix, it identifies a direction where $\mathbf{B}\cdot\mathbf{v}$ is minimized, making it a likely solution for $\mathbf{B}\cdot\mathbf{v} = 0$. In this case, 300 frequency samples were used. Even if the number of samples is increased, the conventional solution remains oscillatory, indicating that the issue is not related to sampling. According to [25], in dynamic systems, especially those described by parameter-dependent matrices, there is a possibility of coalescence, where two or more eigenvalues approach each other to the point that they eventually become identical.

In situations like these, conventional methods, such as QR-based algorithms, may not compute the eigenvectors correctly, resulting in oscillations in the transient simulation [26]. In cases involving one parameter-dependent matrices, such as frequency, eigenvalues are expected to be very close to each other, but they are not expected to coalesce. In this particular case, the possibility of near coalescing may occur [25]. Fig. 13 illustrates the behavior of the seven eigenvalues versus frequency, with markings indicating points where two or more eigenvalues have very close absolute values. In these cases, a tolerance of 10^{-10} was applied. If the tolerance is reduced further, no markings are displayed on the graph.

Finally, Table VI presents the simulation time and the results for the Mean Relative Error of the conventional method compared to the proposed method. It is evident that adopting the SVD method does not compromise computational performance, as the simulation is completed within a few seconds. Furthermore, the total MRE was calculated by considering the largest individual MRE for each element of the seventh column of the matrix.

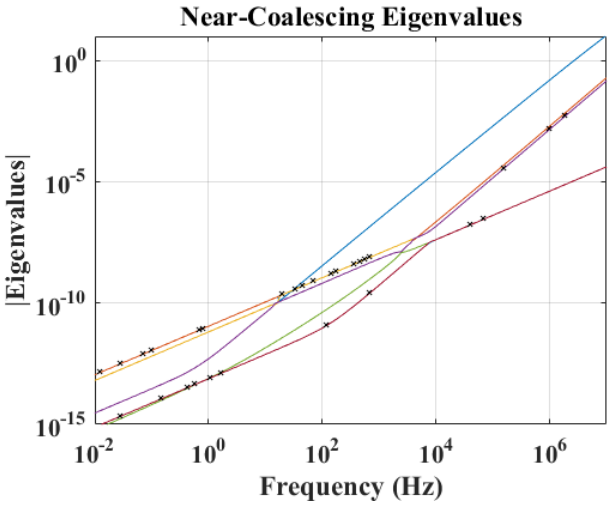

Fig. 13. Near-coalescing eigenvalues.

TABLE VI
SIMULATION TIME AND MEAN RELATIVE ERROR (MRE)

-	SVD	Conventional
Total Simulation Time	3.92s	3.27s
MRE (H)	-	12.574414
MRE (Y_c)	-	4.955714

V. CONCLUSIONS

This work aimed to propose and implement two distinct methods for computing the parameters required for simulating

electromagnetic transients in submarine cables, namely, per-unit-length impedance and admittance, as well as propagation constant and characteristic admittance. The results demonstrate that both methods are valid alternatives, primarily due to their performance in terms of accuracy and their low computational cost.

Regarding the calculation of ground-return parameters, analytical equations that do not rely on integration can be very accurate. However, in cases where the applicability limits are exceeded, it is necessary to identify appropriate methods for calculating the integrals. The optimized DE method is a good option, as it can handle integrals with integrands that contain non-smooth functions. Such cases may arise depending on the parameters defining the propagation medium or even the geometric parameters of the cables. Moreover, it is easy to implement and does not require high computational cost. Additionally, the proposed DE methodology is independent of built-in functions and easy to implement, unlike the global quadrature used for comparison in this study.

Furthermore, SVD can be used instead of methods that cannot provide accuracy and are limited in terms of computational cost. The main advantage of this technique is its robust handling of situations involving particularities such as the possibility of eigenvalue coalescence, as it allows for more direct control over numerical approximation errors. The proposed solution is also easy to implement and is especially useful for ill-conditioned systems.

VI. Appendix

The procedure for applying the Double Exponential formula to Equations (5) and (6) involves the following steps:

1) Apply the interval transformation $\lambda = \frac{x+1}{x-1}$, which changes the integration interval from 0 to ∞ to -1 to 1, rewriting the integral in the format suggested by (12). This substitution redefines the integrand in terms of x;

2) Perform the variable substitution $d\lambda = \frac{-2dx}{(x-1)^2}$, based on the expression suggested in step 1. Define the range of k and the step size h based on the flowchart presented in Fig. 1;

3) Following Equation (12), let $f(x)$ be defined as the integrand of Equations (5) and (6), excluding the constant terms. For each term in the summation, x_k is determined from Equation (13) and w_k from Equation (14). Once these are defined, $f(x_k)$ is calculated, and the summation is computed. Note that (13) and (14) yield constant terms for each value of k with a predefined step size h.

VII. References

[1] A. Ametani, H. Xue, T. Ohno, H. Khalilnezhad, Electromagnetic Transients in Large HV Cable Networks: Modeling and Calculations, vol. I. London: IET Press, 2021, p. 1-2.

[2] N. Jiang, C. Yang, H. Xue, J. Mahseredjian, "An investigation of electromagnetic transient characteristics on a practical 500 kV submarine cable system," Electric Power Systems Research, vol. 223, pp. 1-2, Oct. 2023.

[3] W. Wang, G. Li, J. Guo, "Large-Scale Renewable Energy Transmission by HVDC: Challenges and Proposals," Engineering, vol. 19, pp. 252-267, Dec. 2022.

[4] Y. Xu, Z. Zhao, B. Yue, X. Li, "Research on Transient Overvoltage Characteristics of VSC-HVDC Transmission System Connecting to Large-scale Offshore Wind Farm," in 4th International Conference on HVDC, pp. 443-448.

[5] F.A. Uribe, O. Ramos-Leaños, P. Zuniga, "An investigation of earth and sea-return impedances of power electrical cables," Electric Power Systems Research, vol. 223, pp. 1-2, Oct. 2023.

[6] A. Ametani, "A General Formulation of Impedance and Admittance of Cables," IEEE Transactions on Power Apparatus and Systems, vol. PAS-99, No. 3, pp. 902-910, Jun. 1980.

[7] T.A. Papadopoulos, D.A. Tsiamitros, G.K. Papagiannis, "Earth return admittances and impedances of underground cables in non-homogeneous earth,", IET Generation, Transmission Distribution vol. 5, pp. 161-171, Jul. 2010.

[8] H. Kr. Høidalen, "Analysis of Pipe-Type Cable Impedance Formulations at Low Frequencies," IEEE Transactions on Power Delivery, vol. 28, pp. 2419-2427, Oct. 2013.

[9] G. Di Lorenzo, E. Stracqualursi, M. Marzinotto, J. Brandão Faria, R. Araneo, "Ground-Return Parameters of Submarine Cables Buried in the Seabed," IEEE Transactions on Electromagnetic Compability, vol. 65, pp. 574-584, Apr. 2023.

[10] H. Xue, A. Ametani, J. Mahseredjian, J, I. Kocar, "Generalized formulation of earth-return impedance/ admittance and surge analysis on underground cables," IEEE transactions on power delivery, vol. 33, pp. 2654–2663, Dec. 2018.

[11] J. C. L. V. Silva, A. C. S. Lima, A. P. C. Magalhães, M. T. C. de Barros, "Modelling seabed buried cables for electromagnetic transient analysis," IET Generation, Transmission Distribution, vol. 11, pp. 1575-1582, Apr. 2017.

[12] A. Cywiński, K. Chwastek, "Modeling of skin and proximity effects in multi-bundle cable lines," in Proc. 2019 Progress in Applied Electrical Engineering (PAEE), pp. 1-5.

[13] U. R. Patel, P. Triverio, "MoM-SO: a Complete Method for Computing the Impedance of Cable Systems Including Skin, Proximity, and Ground Return Effects", IEEE Transactions on Power Delivery, vol. 30, pp. 2110-2118, Oct. 2015.

[14] J. Morales, H. Xue, J. Mahseredjian, I. Kocar, "A New Tool for Calculation of Line and Cable Parameters," Electric Power Systems Research, vol. 220, pp. 1-8, Jul. 2023.

[15] A. De Conti, N. Duarte, R. Alipio, "Closed-form expressions for the calculation of the ground-return impedance and admittance of underground cables," IEEE transactions on power delivery, vol. 38, pp. 2891–2900, Aug. 2023.

[16] T. Worzyc. Submarine Power Cables Design: Installation, Repair, Environmental Aspects, vol. I. Heidelberg: Springer, 2009, p. 6-7.

[17] C. Liu, "Comparison and Selection of Three-Core Cable and Single-Core Cable," in IOP 2019 Conference Series: Earth and Environmental Science, pp. 1-4.

[18] F. Pollaczek, "Sur le champ produit par un conducteur simple infiniment long parcouru par un courant alternatif," Revue Gén, Elec., vol. 29, pp. 851-867, Apr. 1931, (in French).

[19] L.M. Wedepohl, D.J. Wilcox, "Transient analysis of underground power-transmission systems. System-model and wave propagation characteristics," Proceedings of the Institution of Electrical Engineers, vol. 120, pp. 253-260, 1973.

[20] H. Takahasi, M. Mori, "Double Exponential Formulas for Numerical Integration," Publications of the Research Institute for Mathematical Sciences, vol. 9, pp. 721-741, Aug. 1974.

[21] M. Mori, "Discovery of the Double Exponential Transformation and Its Developments," Publications of the Research Institute for Mathematical Sciences, vol. 41, pp. 897–935, Nov. 2005.

[22] R. A. van Engelen. (2021, Jun.). Improving the Double Exponential Quadrature Tanh-Sinh, Sinh-Sinh and Exp-Sinh Formulas. Genivia Labs, New York, NY. [Online]. Available: https://www.genivia.com/qthsh.html

[23] M. Capobianco, G. Criscuolo, "The stability of the gauss-laguerre rule for cauchy p.v. integrals on the half line," American Journal of Computational Mathematics, vol. 13, pp. 505–511, Dec. 2023.

[24] J. Bisgard, Analysis and Linear Algebra: The Singular Value Decomposition and Applications, vol. I. Providence: AMS, 2021, p. 123-126.

[25] W. Beyn, L. Dieci, N. Guglielmi, E. Hairer, J. Sanz-Serna, M. Zennaro, Current Challenges in Stability Issues for Numerical Differential Equations, vol. I. Cetraro: Springer, 2011, p. 173-178.

[26] L. Wedepohl, H. Nguyen, G. Irwin, "Frequency-Dependent Transformation Matrices for Untransposed Transmission Lines using Newton-Raphson Method," IEEE transactions on power systems, vol. 11, pp. 1538–1546, Aug. 1996.